SUPERCONDUCTING REBALANCE ACCELEROMETER*

R. P. Torti, M. Gerver, K. J. Leary, S. Jagannathan, D. M.Dozer
SatCon Technology Corporation
Cambridge, MA

SUMMARY

A multi-axis accelerometer which utilizes a magnetically-suspended, high-T_c proof mass is under development. The design and performance of a single axis device which is stabilized actively in the axial direction but which utilizes ring magnets for passive radial stabilzation is discussed. The design of a full six degree-of-freedom device version is also described.

INTRODUCTION

There have been a number of instruments developed which utilize levitation of a superconducting proof mass as the basis for sensing acceleration and gravity gradients[1,2,3,4]. The advantages of these approaches at liquid-helium temperature include reduction of electrical and mechanical fluctuations by a factor of 10, while superconducting operation implies negligible dissipation from current carrying elements. Use of instrumentation such as SQUIDs which depend upon significant quantum effects at low temperatures becomes practical. Furthermore, the flux trapping properties of superconductors allows stable field control. For applications such as gravimeters, where the devices must detect small changes against a 1 G background, a superconducting coil can be used to levitate the proof mass with high long term stability since a low decay rate persistent current in the levitation coil is used to cancel gravity[1].

A serious disadvantage with conventional superconductors is the requirement to cool to 4.2 K which is both expensive and requires more volume relative to operation at 77 K. The use of high-T_c materials does not retain all the advantages of conventional superconductors, but nonetheless brings with it lower than room temperature thermal noise, insignificant electrical power dissipation in coils, and the advantages of flux trapping.

This work was approached as an examination of the feasibility for using a superconducting proof mass in conjunction with low noise displacement sensors in the development of a multi-axis acceleration sensor. Major efforts were undertaken along three lines: 1) Development of an extremely low-noise displacement sensor operating at RF frequency, 2) testing of a one degree-of-freedom test device which uses a high-T_c proof mass and 3) design and operation of full 6 degree-of-freedom proof-of-principle multi-sensor.

---

*Work done on contract for NASA Langley Research Center, NAS1-19938.

APPROACH

The conceptual design is for a multi-sensor which detects linear and angular acceleration along six axes. In operation, a measurement of the displacement of a fully magnetically-suspended mass is detected in conjunction with an active control system which "rebalances" to the original position. The necessary drive to accomplish this is processed into the corresponding output signal. Use of a rebalance scheme minimizes non-linearities in displacement sensors and actuators. The limited proof-mass motion inherent in a rebalance system also allows more accurate position measurements to be made and improves performance. A suspended proof-mass device, while more complex than spring-restraint systems, has the further advantage of active control of the different stiffness and damping characteristics at different frequencies. This allows better vibration isolation from external disturbances.

A conceptual drawing of the sensor is shown in Figure 1. It consists of a cubically shaped high temperature superconducting proof-mass whose position is sensed and controlled by a set of co-located capacitive sensors and control coils fixed to a support structure cooled to liquid nitrogen temperature. The control coils are actuated by an electronic control system to maintain a constant cube position based upon outputs from displacement sensors. From the mass dynamics of the cube and the actuator control signals, three accelerations and three angular rates can be determined. In this prototype, six sensors and actuators are sufficient to control the six degrees-of-freedom of the cube although other workers have used more for averaging and redundancy[4]. The cube, sensors, and control coils are contained in an evacuated vessel with the coils and sensors mounted to the internal cooled support jacket.

The device has several features that should enhance performance. First, high frequency capacitive sensors can yield position sensitivities of 10^{-3} angstroms/$\sqrt{Hz}$. Second, the proof mass, sensors and coils are cooled to 77 degrees Kelvin which reduces mechanical thermal noise to approximately half that at room temperature. Third, the use of a superconducting 1 G levitation coil generates very little heat in the system, reducing thermal gradients which would degrade precision. Fourth, operation at 77 K brings with it the possibility for substitution of a bulk high-T_c material disc for the wire coil. This "coil" could be charged inductively and operated persistently.

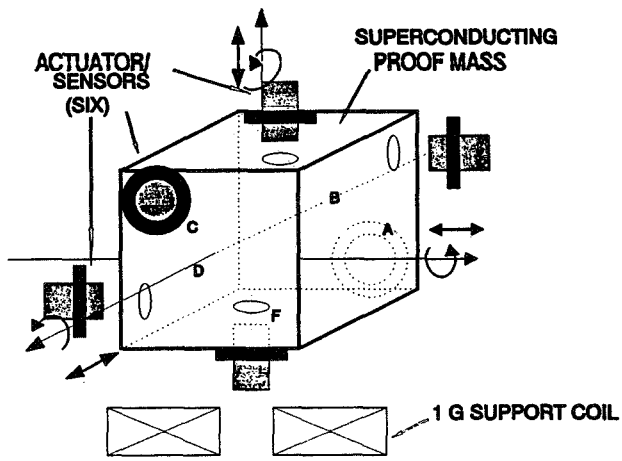

Figure 1. Schematic of Multi-sensor Illustrating Principle of Operation.

Configured in this optimal way, the device would have stand alone resolution of 0.1 μg acceleration and 10^{-5} rad/sec^2 angular acceleration and would drift 75 angstroms and 5 x 10^{-5} degrees in one hour due to sensor noise. These numbers are based on a bandwidth of 100 Hz, the use of capacitive position sensors with noise of 1.5 x 10^{-3} Å/$\sqrt{Hz}$ and a cube of diameter 2 cm. The drift is assumed to be a random walk, with time step ($10^{-2}/2\pi$) seconds, and spatial step equal to the sensor noise at 100 Hz. Any systematic (non random) drift would be in addition to drift from sensor noise.

ONE DEGREE-OF-FREEDOM TEST DEVICE

The design of the full multi-sensor accelerometer involves the integration of at least three demanding technologies: bulk and wire superconductor fabrication, cooling with liquid cryogens through a vacuum, and active electronic control. Especially significant for latter are flux pinning and hysteretic effects observed in high-T_c materials, which can make the operating point dependent upon magnetizing history affecting both magnetic spring constant and damping.

To provide information for the design of the six degree-of-freedom device, a simpler device involving a fully suspended proof mass but with only one degree-of-freedom has been built and is currently under testing. This is shown in block form in Figure 2. A magnetic geometry is utilized which is passively stable in all directions except axially. Magnetization of ring magnets either normal to their face or radially will produce axially symmetric, radial forces. The sense of the magnetization can be chosen so that the movable element can then be positioned axially so that it is in a radial but not axial potential well. The axial position is then controlled by the active magnetic repulsion generated between the control coil and superconductor and sensed by the displacement sensor.

This is implemented as shown in Figure 3. For mechanical simplicity, sensing functions have been separated from coil/superconducting disc functions. This is accomplished by attaching the proof mass, ring magnets and sensor target to a rod which is part of the suspension. At its top the proof mass is completely re-entrant into the liquid nitrogen reservoir. Dual magnet rings sets are incorporated for alignment stability. This arrangement will also allow maximization of the vacuum gap between cold regions and vessel walls with sensor at room temperature. The entire support assembly is placed in a "bell jar" consisting of a Nalgene cover and stainless steel base plate. Liquid coolant is forced through a copper baffle into the stainless reservoir by tank-pressurized liquid nitrogen. A vent to the liquid chamber allows access for vacuum pumping to decrease temperature below 77 K. With the superconducting and suspended proof mass re-entrant into the reservoir and facing the cold baffle below, effective cooling has been achieved.

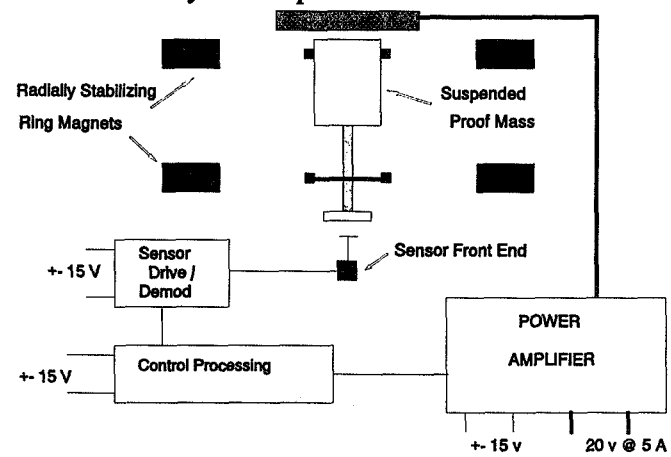

Figure 2 Block diagram of single-axis device.

Test Device Sizing

The mass is sized at about 75 gm to correspond to the full 6 degrees-of-freedom cube. The two sets of permanent magnets are mounted in such a way that only one degree-of-freedom (vertical motion) will be unstable, while the horizontal motion and tilting degrees of freedom are stable. If the vertical separation distance between the two sets of rings is at least a few times the radial separation

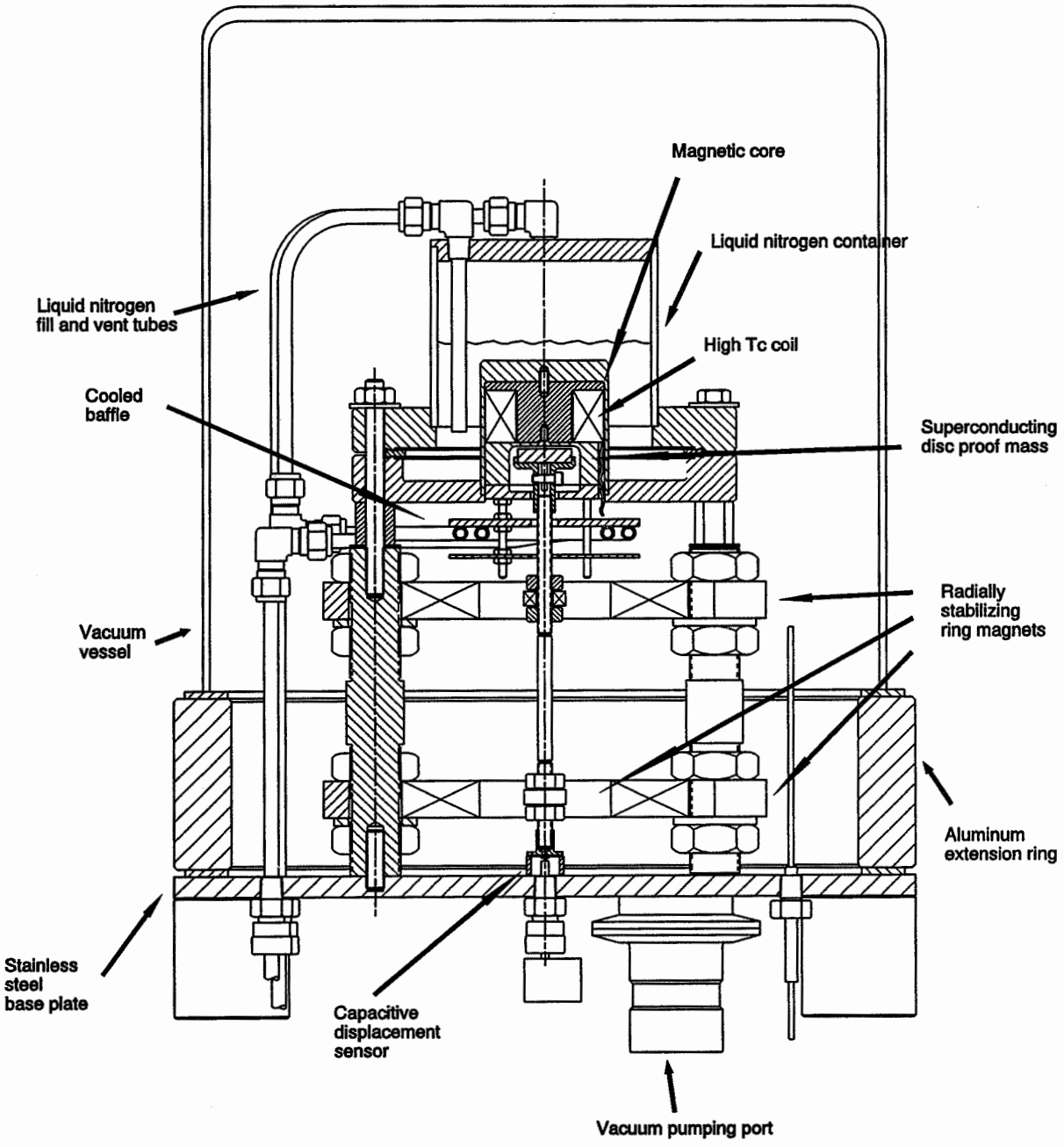

Figure 3. One degree-of-freedom test device.

within each set, then the two sets will not exert appreciable forces on each other.

The rings of each set are magnetized vertically with radial thickness w_i and w_o for the inner and outer rings, average radius r_i and r_o, and height h_i and h_o (see Figure 4). The forces between the inner and outer rings may be calculated by assigning an effective magnetic monopole surface charge to the top and bottom surfaces of each ring and integrating the forces, assuming that the force between two magnetic monopole charges q_1 and q_2, separated by a distance r. It is given by

$$F = q_1 q_2 / 4\pi\mu_0 r^2$$

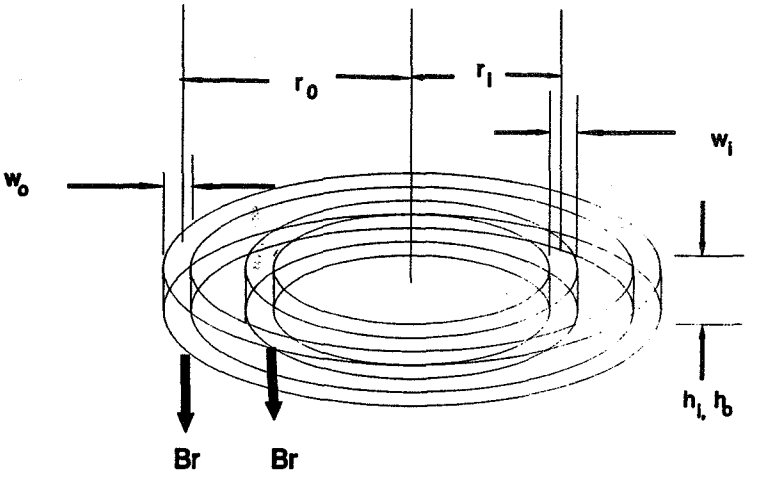

Figure 4. Magnet geometry.

in analogy to electrostatic forces. The effective magnetic charge density is then equal to the divergence of the intrinsic magnetization, which is always close to B_r, regardless of the magnet dimensions, for rare earth magnets. So the magnetic surface charge is B_r for the north pole surface of each ring, and $-B_r$ for the south pole surface. The forces take a particularly simple form if

$$w_o, w_i \ll \max(r_o - r_i, |h_o - h_i|) \ll r_o, r_i$$

Then, if the inner and outer magnets are both magnetized in the same direction, we find the vertical spring constant for one set of rings is

$$\frac{\partial F_z}{\partial z} = \frac{B_r^2}{\mu_0} w_i w_o (r_i + r_o) \left(\frac{(r_o - r_i)^2 - (h_o - h_i)^2/4}{[(r_o - r_i)^2 + (h_o - h_i)^2/4]^2} - \frac{(r_o - r_i)^2 - (h_o + h_i)^2/4}{[(r_o - r_i)^2 + (h_o + h_i)^2/4]^2} \right)$$

$$\frac{\partial F_x}{\partial x} = \frac{\partial F_y}{\partial y} = -\frac{1}{2}\frac{\partial F_z}{\partial z}$$

To suspend a 70 gm proof mass with a 0.5 cm displacement between the magnet sets the required spring constant is

$$\frac{70g \times 9.8 m/\sec^2}{0.5\ cm} = \frac{7 \times 10^2 \times 9.8}{5 \times 10^{-3}} = 1.4 \times 10^2 N/m$$

for each ring.

It can be shown that similarly sized rings with small radial spacings make too stiff a spring. Making magnets much smaller, or making $(r_0-r_i) \approx (h_0-h_i)$, makes the spring constant very sensitive to dimensions and position while making w_0, w_i much smaller is difficult mechanically.

A soft enough spring can be achieved with low intensity (B_r) magnets and large radial spacings. Ceramic magnets with $B_r \approx 0.38$ tesla were used with:

$$w_0 = 3.5 \text{ cm}, w_i = 0.6 \text{ cm}, r_i = 0.6 \text{ cm}, r_0 = 4.7 \text{ cm}, h_i = 0.6 \text{ cm}, \text{ and } h_o = 1.6 \text{ cm},$$

This gives a spring constant $\approx$ 110 N/m per ring set which can easily support approximately 100 gm of proof mass and magnets over an axial range of 0.5 cm.

Superconductors

Two high-T_c superconducting components are used in this device. A single fixed coil provides both bias against the magnetic spring and active control while the suspended proof mass comprises a ring magnet support rod, the sensor target, and disc of bulk YBCO which interacts with the coil to produce a repulsive (levitating) force. The sole rationale for the coil was minimization of a heat source close to the levitated superconductor since a coil/core set capable of canceling 1 G dissipates approximately 40 W.

The coil, fabricated by American Superconductor Co. of Westborough, MA, operates in zero background field at 77 K at 3000 Amp-turns. Coil size is approximately 53 mm outside diameter 23 mm long with a 25 mm bore. The superconductor is Lead Bismuth Strontium Calcium Copper Oxide. The coil dissipates ~0.04 W at full current.

The suspended disc is a 25 mm diameter by 6.4 mm thick "YBCO large-domain levitator" fabricated by Superconductive Components, Inc. of Columbus Ohio.

Displacement Sensing

The initial multi-sensor concept device included operation in conjunction with fast, high precision capactive placement sensors. For shot noise limited resolution, the fractional position sensitivity limit is

$$\delta d/d = \sqrt{(2e/I)} \cdot (\sqrt{Hz})^{-1}.$$

Here I is the bias current and the electronic charge. δd can be reduced by increasing the drive frequency which is the rationale for high frequencies.

Although the current multi-sensor is designed primarily for proof-of-principle operation due to cost constraints, and not optimized for precision or bandwidth, a single high-precision RF driven

capacitive displacement sensor prototype was designed, built and tested. The sensor is based upon circuity designed by RCA[5] for capacitive video disc reader. The principle has also been developed by a group at JPL[6].

As conceived by RCA, a drive signal of nearly 1 GHz is imposed upon a resonator which includes the capacitance of the electrode gap to be measured. Displacement is read as a change in RF tune since the detected signal amplitude moves along the tuning curve as the resonance frequency changes. Sensitivity is enhanced by operation around the sharp slope of the resonance curve. Active control via a voltage controlled oscillator (VCO) fixes the operating point. Unlike the RCA implementation, which used stripline technology, this design employs a miniature coaxial cable as both transmission line and resonator.

Resonant frequency and Q were determined by measurement of the AC amplifier output voltage vs. frequency with the modulators disabled and 10% AM on the master oscillator output. The quantity dV_o/df (derivative of operating point voltage with frequency) was measured by changing the master oscillator frequency with the modulator operating and measuring the DC output of the 1.0 kHz low pass filter. The master oscillator, an HP8656B capable of $1:10^8$ in frequency, provides oscillator drive and frequency readout. The peak-to-peak noise was estimated by an oscilloscope from the filter output. Auxiliary measurements of V_o and/or oscillator frequency for null V_o were taken for various test capacitor plate separations, recorded as actuator micrometer readings.

The measured dV_o/df was combined with a simulated model of the resonator to compute a V_o/C, in volts/pF, which was then used to compute a noise equivalent capacitance change from the measured noise. With 2mm x 2mm plates and 0.1 mm spacing, the nominal capacitance is 0.35 pF and separation sensitivity about 3.5×10^{-9} F/m. Dividing the noise equivalent capacitance by this number gives an rms position error of 2.5×10^{-11} m (2.5×10^{-12} m/$\sqrt{\text{Hz}}$). In a 100 Hz bandwidth this is approximately a sensitivity in acceleration 1×10^{-5} m/s^2 or 10^{-6} g.

Force Calculations

In order to limit the size and expense of the superconducting suspension coil, it was found necessary to include a soft magnetic core and optimize core and coil geometry with finite element calculations. Calculated levitation forces produced by a permanent magnet and melt-process YBCO levitators were higher by about a factor of 2.5 compared to data provided by Superconducting Components, Inc. This was discrepancy was corroborated by measurements at SatCon and included in core and coil sizing designs.

Control

The operation of the multi-sensor is based on measurement of forces and moments required to restore the proof mass, i.e., the superconducting cube, to a center zero orientation. A

force/moment rebalance controller with a displacement feedback is the basis for achieving this measurement. The principle is illustrated with a single degree-of-freedom force rebalance system as shown in Figure 5.

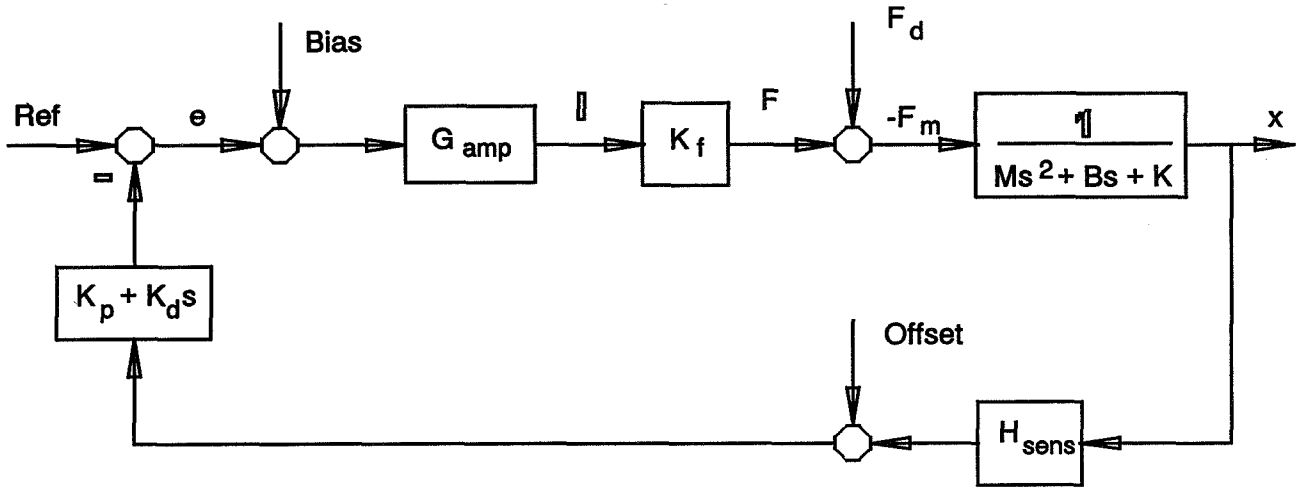

Figure 5. One axis, closed-loop control block.

Closed Loop Design

The controlled system is closely approximated by a second-order system of mass M, equivalent viscous damping B, and stiffness K. The equivalent viscous damping occurs as a result of the motion of pinned flux. This pinned flux is also responsible for a portion of the overall system stiffness K.

The overall system stiffness has contributions from two equivalent spring constants. The first contribution results from the interaction between permanent magnets mounted on the proof mass and the stationary dewar. Ideally, the system can be stabilized at this (unstable) equilibrium point and the contribution to the overall spring rate is zero. However, in practice, a negative contribution to the overall rate is observed. The second contribution to the overall spring rate is due to flux pinning which allows the proof mass to be stabilized at an otherwise unstable equilibrium point.

The block diagram illustrates the closed-loop system. Both a control force F_e and a disturbance force F_d may be applied to the multi-sensor proof mass. The disturbance force is proportional to the acceleration of the multi-sensor. In a suitably small neighborhood of the operating point, the control force is proportional to the applied current through the force constant K_f. A current controlled amplifier with adjustable gain G_{amp} is used to provide a current proportional to the compensated error signal e. Displacement feedback is received through the frequency dependent gain H_{sens}.

Since the system closely resembles a second order oscillator, the simplest stabilizing controller is a proportional plus derivative (PD) controller. As shown in the figure, proportional K_p and derivative K_d gain terms appear in the feedback path. In theory, this control structure allows

independent control of the system damping and stiffness through the adjustment of K_d and K_p, respectively. The compensated error signal is proportional to the required restoring force and may be used for the sensor output.

The closed-loop transfer functions of merit are given below.

$$\frac{x(s)}{F_d(s)} = \frac{1}{Ms^2 + (B + G_{amp}K_fH_{sens}K_d) + (K + G_{amp}K_fH_{sens}K_p)}$$

$$\frac{e(s)}{F_d(s)} = \frac{-H_{sens}(K_{dS} + K_p)}{Ms^2 + (B + G_{amp}K_fH_{sens}K_d) + (K + G_{amp}k_fH_{sens}K_p)}$$

Controller Implementation

A practical analog implementation of the control circuit is shown in Figure 6. A practical differentiator is constructed from an LM318. For stability and noise reduction, second order poles are placed at 270 and 330 Hz. Inverting gain stages provide variable derivative and proportional gains for damping and stiffness adjustment. A unity gain inverting summer provides a variable reference and produces the compensated error signal used to drive the adjustable gain current amplifier.

Performance

Open-loop frequency scans of proof-mass displacement at constant forcing current indicate a peak with highly non-linear behavior between 10 and 20 Hz which is in the range of the resonance expected with the designed magnetic spring and measured proof mass. Current efforts involve observing the effects of varying ring magnet alignment, the level of frozen-in flux, and circuit gains on closed loop performance.

SIX DEGREE-OF-FREEDOM PROTOTYPE

The multi-axis device has six degrees of freedom, namely x,y,z translation and θ_x, θ_y, and θ_z rotations as shown in Figure 7. The actuator coils and capacitive sensors are collocated. There can be one or two sensors and actuators reacting against each face of the cube shaped proof mass (six or twelve total). Each actuator coil and sensor pair is located on a diagonal of the face. The cube faces are identified as A,B,C,D,E,F with the corners defining the faces. By virtue of the location of the actuator coil/sensor pair, each pair can generate a force along one translational axis and a moments around two rotational axis. If the forces generated by the actuator coils are defined by a vector

$$F_{act} = [F_a, F_b, F_c, F_d, F_e, F_f]^{-1}$$

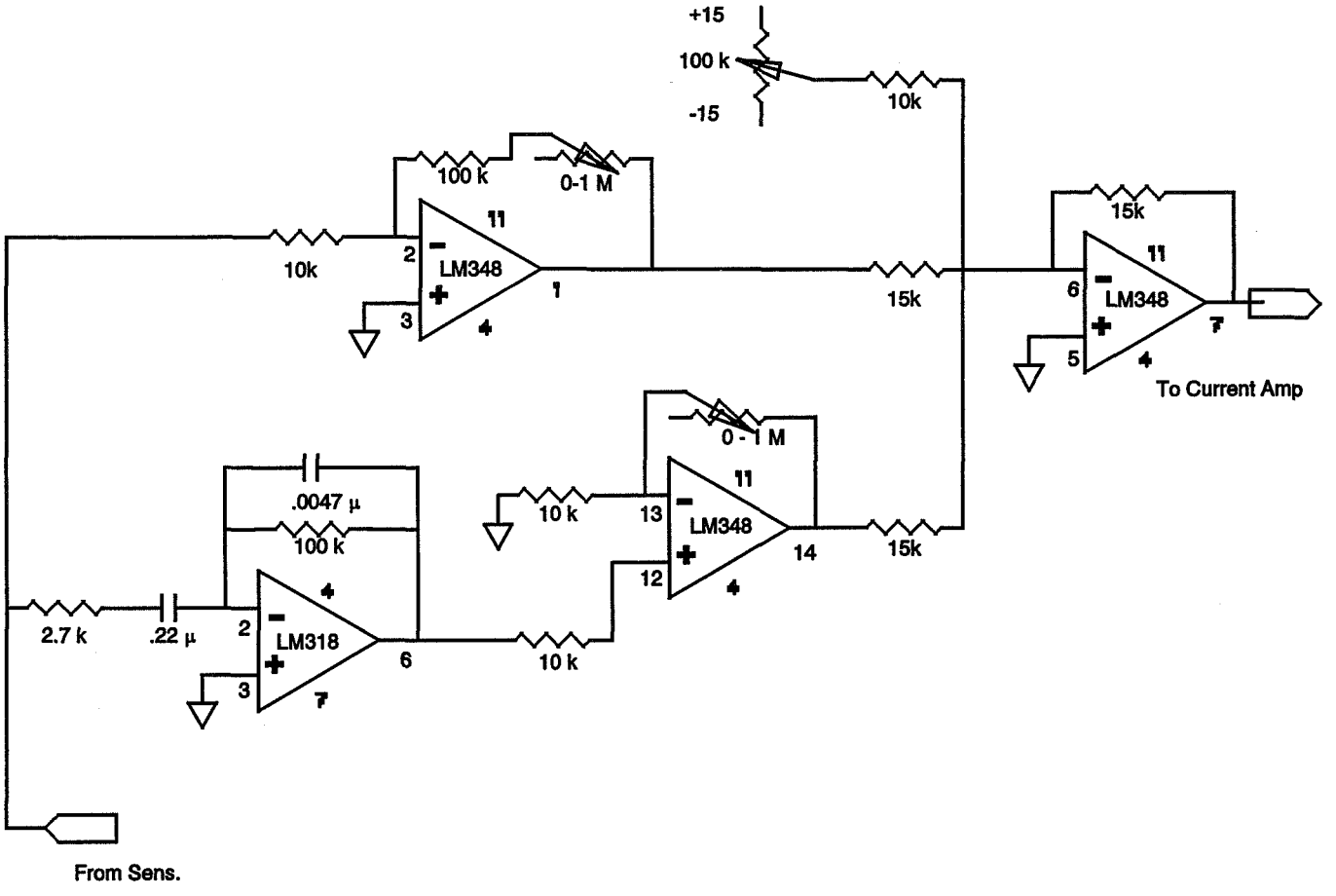

Figure 6. Single axis electronics implementation.

then a transformation can be found which relates F_{act} the forces and moments

$$FM = [F_x, F_y, F_z, M_x, M_y, M_z]^{-1} = [T]*F_{act}$$

As the sensors are collocated with the actuator coils, the displacements measurement "d" at each sensor can be transformed to translations and rotations using the same matrix [T], i.e.,

$$[X, Y, Z, \theta_x, \theta_y, \theta_z]^{-1} = [T][d_a, d_b, d_c, d_d, d_e, d_f]^{-1}$$

Use of the transform [T] and $[T]^{-1}$ allows the controller to be six decoupled compensators, one for each degree-of-freedom. The compensation is then tailored to meet the frequency response requirements of the sensor system.

A functional block of the multi-axis device is shown in Figure 8. Six displacement sensors are used in conjunction with six normal control coils. A single superconducting coil is used to continuously cancel 1 G of the proof mass. The normal control coils operating at 77 K produce about 4 W when

rebalancing 0.3 G.

The mechanical implementation of this device is shown in Figure 9. The vacuum vessel configuration is the same as the single axis test device. The liquid nitrogen container is of aluminum, bored for six sensor/coil pairs entering the shell at oblique angles. Steel magnetic cores are used to tailor the fields. The 1 G support coil is imbedded in the base of the container and faces upward to repel the cubical proof mass oriented vertically along an axis which includes a set of diagonally opposed vertices.

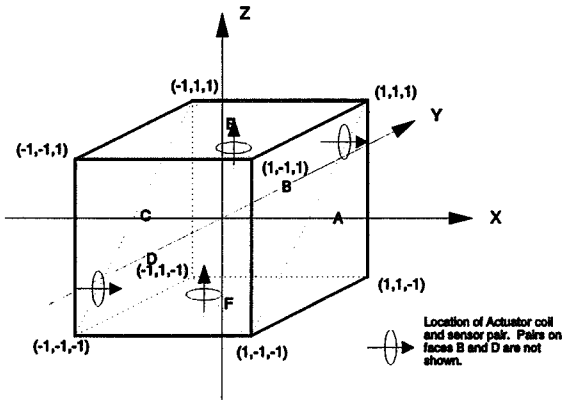

Figure 7. Sensor and actuator location nomenclature.

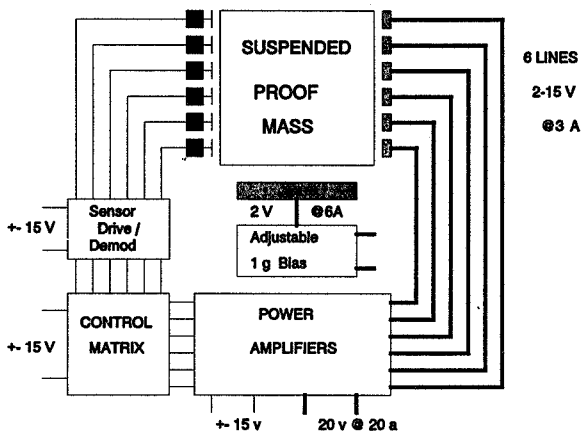

Figure 8. Block of six degree-of-freedom prototype.

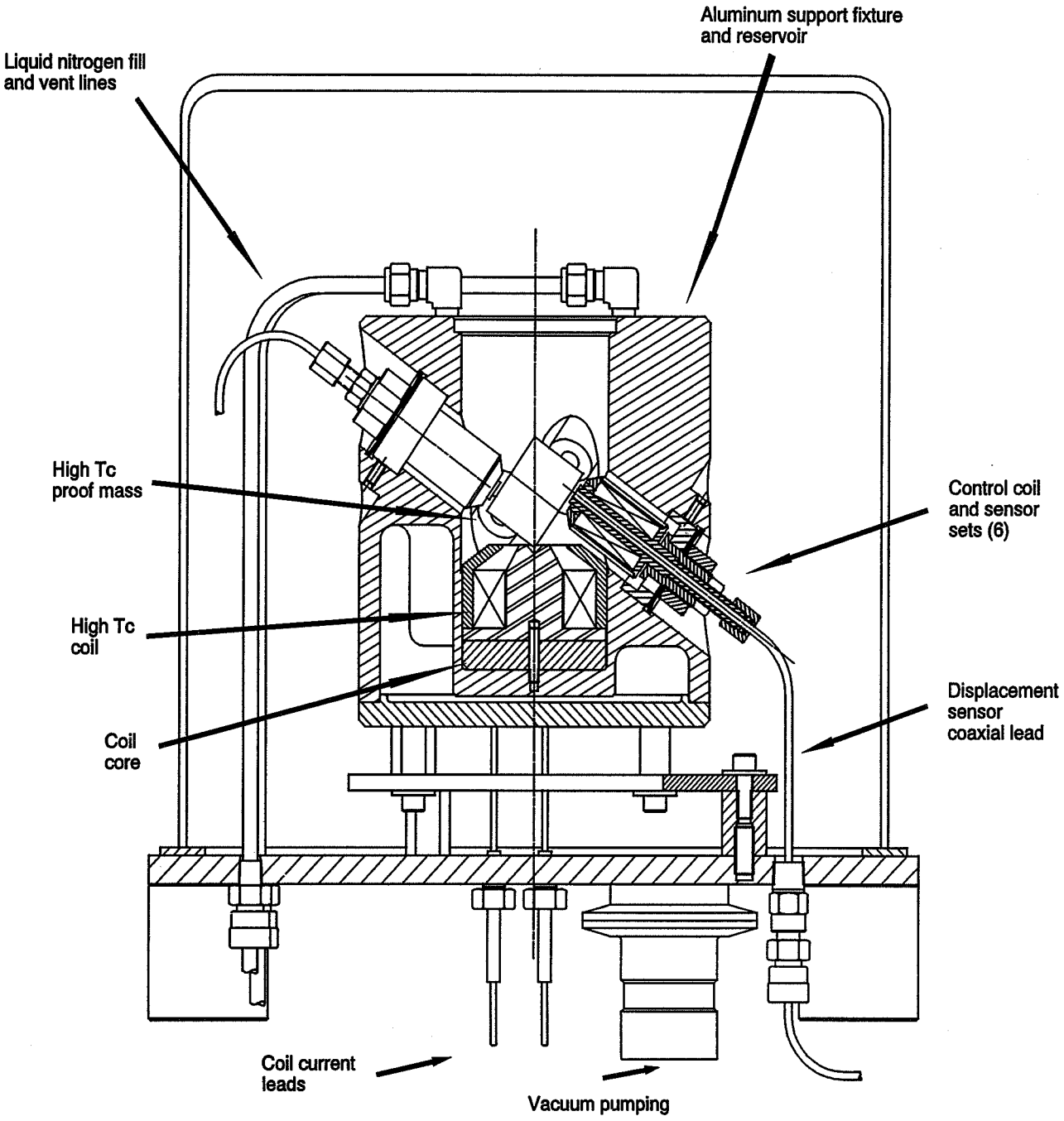

Figure 9. Six degree-of-freedom test device.

REFERENCES

1. J. M. Goodkind and R. J Warburton, "Superconductivity Applied To Gravimetry," IEEE Trans. on Magnetics, **MAG-11**, 708 (1975).

2. J.M. Goodkind, P.V. Czipott, A.P. Mills,Jr., M. Murakami, P.M. Platzman, C.W. Young, D.M. Zuckerman, "Test of the Gravitational Inverse-square Law at 0.4 to 1.4 m Mass Separations," Phys. Rev. D, **47**, 1290 (1993).

3. M.V. Moody and H.J. Paik, "Gauss's Law Test of Gravity at Short Range," Phys. Rev. Lett. **70**, 1195 (1993).

4. Ho Jung Paik, Edgar R. Canavan, Benjamin Backrach, Hans J Haucke, "Development of Superconducting Technology for Inertial Guidance, Gravity Survey, and Fundamental Gravity Experiments," Report PL-TR-94-2222, (1994).

5. R.C. Palmer, E.J. Denlinger, and H. Kawamoto, "Capacitive-Pickup Circuitry for VideoDiscs," RCA Review **43** 194 (1982).

6. T. R. Van Zandt, T. W. Kenny, W. J. Kaiser, "Ultra-High-Frequency Capacitive Displacement Sensor," NASA Tech Briefs, **18** (1994) 42.